Quantum Transport

1. Introduction

In conventional electronic devices such as field-effect transistors (FETs) or diodes, the size of the device is usually quite large, so that the wave nature of the electron or its discrete charge do not influence the behavior of the device. Furthermore, all individual components of these devices are of a size much larger than an individual atom. However, with the continuous shrinking of integrated circuits, novel effects will arise at the nanoscale: Contemporary FETs are already now approaching the length scales in which some of the transistor's parts are scaled down to atomic dimensions. For example, the width of the channel of a state-of-the art FET is only about 35 nm (**Figure 1**) and the thickness of the gate insulator is only few atoms thick (inset to **Figure 1**). The outlook what a commercial FET might look like is already in a development stage nowadays. For example Singh et al.[2] could show that by process techniques that are also used in industry, working silicon nanowires FETs with channels composed only of a 3 nm silicon nanowire can be fabricated (**Figure 2a**). At low temperatures, they were able to see significant fluctuations in the current flowing through the transistor (**Figure 2b**) as a function of the gate-source voltage. These fluctuations are due to single-electron charging effects, as will be explained in the remainder of this chapter. Before we come to the description of phenomena in electric transport that only appear when electrons are confined to small dimension, we will discuss the basics of the conventional FET, as it is the basis for many of the phenomena described in the following.

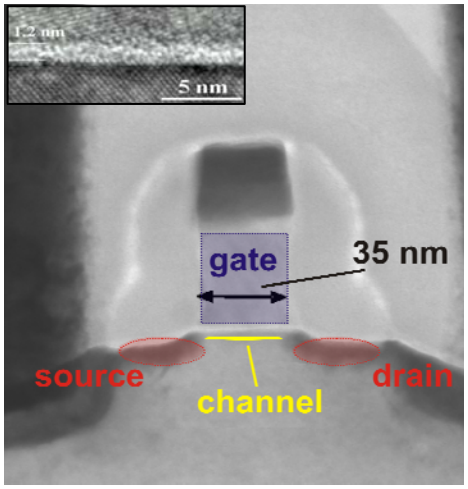

Figure 1: Scanning electron microscopy (SEM) image of a contemporary field-effect transistor (FET). (Inset) Transmission electron microscopy (TEM) image of a gate insulator (source: Intel).

2. Basics of field-effect transistors (FETs)

A transistor is a semiconductor device commonly used to amplify or switch electronic signals. A transistor is made from a solid piece of semiconducting material, with at least three terminals for connection to an external circuit. A voltage or current applied to one pair of the transistor's terminals changes the current flowing through another pair of terminals. Because the controlled (output) power can be much larger than the controlling (input) power, the transistor provides amplification of a signal. The transistor is the fundamental building block of modern electronic devices, and is used in radio, telephone,

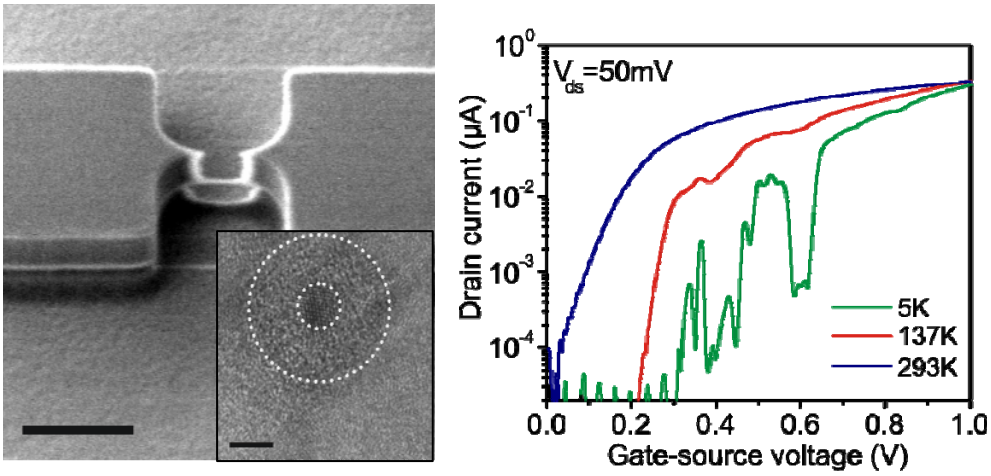

Figure 2:(a) SEM image of a nanowire FET fabricated with conventional CMOS-compatible techniques (scale bar 500 nm). The diameter of the nanowire is only 3 nm. (**inset**) TEM image of the channel showing the nanowire (scale bar 4 nm), the wrap-around gate dielectric (SiO_2). (b) Transfer curve of the FET showing confinement of the charge carries effects at low temperatures (Figure adopted from Ref 2).

computer and other electronic systems. Modern transistors are usually so called field-effect transistors (FETs) in which the transistor action is steered via an electric field, hence the name. The first metal-oxide-semiconductor FET (MOSFET) was realized in 1960 by Kahng and Atalla[8]. The schematic structure of a MOSFET is shown in **Figure 3**. The semiconducting channel is connected to two terminals (labeled source (S) and drain (D)) that are used to apply a voltage along the channel, whereas the third terminal (labeled gate (G)) is electrically insulated from the semiconducting channel. It serves to control the electrostatic potential at the semiconductor/insulator interface. The so called gate capacitor is formed by the gate insulator (for example SiO_2) and two electrodes namely the metallic gate electrode on the one side and the semiconductor on the other. A phenomenological explanation of the operation of a FET is that by the application of for example a positive voltage to the gate electrode, electrons are accumulated on the other side of the gate capacitor, that is in the semiconductor. The accumulated electrons can be pushed through the channel from source to drain by the drain-source voltage. However, in order to for example understand the exponential increase of the current of a FET as the gate voltage is changed, we have to go a bit deeper into semiconductor physics, which we will briefly do in the following.

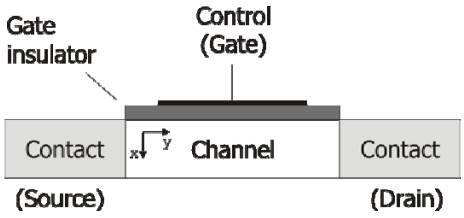

Figure 3 Schematic depiction of a FET.

Doping of a semiconductor

The charge carrier density of the semiconducting material used for the fabrication of the FET can be tailored by appropriate manufacturing techniques according to the necessities of the application. This modification, known as doping of the semiconductor is the process of intentionally introducing impurities into an extremely pure (also referred to as intrinsic) semiconductor to change its electrical properties. The impurities are dependent

upon the type of semiconductor. In order to obtain a *p*-type semiconductor one has to dope the intrinsic semiconductor using acceptor atoms like boron (when Silicon is used as semiconductor) which take up an electron from the semiconductor and leaves an extra hole. This results in a shift of the Fermi level close to the valence band. By doping the intrinsic semiconductor with donor atoms like arsenic (when Silicon is used as semiconductor), one can shift the Fermi level close to the conduction band thus creating an *n*-type semiconductor.

Operation principle of a FET

In FETs, the current through the channel (called the drain current I_D) is modulated by controlling the electrostatic potential of the channel via the application of a voltage between the gate and the source terminal (V_{GS}). In order for this potential change to affect the current through the channel, it has to alter the concentration of charge carriers in the channel. This can easily be seen from the Drude model in which the current is given by

$$I_D \propto \sigma \cdot V_{DS} = n \cdot e \cdot \mu \cdot V_{DS} \qquad (2.1)$$

Here, σ is the conductivity of the channel, n the density of charge carriers in the channel, μ the mobility of the charge carriers, V_{DS} the voltage applied between the source and drain electrode and e the electron's charge. The current I_D flows because of the potential difference V_{DS} between the source and the drain electrode. μ is given by

$$\mu = e \cdot \tau / m^* \qquad (2.2)$$

with τ the time between two scattering events (relaxation time) and m^* the effective mass of the charge carriers. Since μ is usually not affected by the electrostatic potential applied to the gate terminal, the modulation of the drain current results from the modulation of the charge carrier density in the semiconducting channel. To understand this, we consider the change of the charge carrier density in the semiconductor of a FET in the vicinity of the semiconductor/gate insulator interface on the application of a potential ϕ to the gate electrode. In a p-doped semiconductor for example, the density of holes p in the valence band depends exponentially on ϕ and is given at low temperatures by [9]

$$p_\phi(x) = \frac{N_V n_A}{n_D} \cdot \exp\left(-\frac{E_a}{k_B T}\right) \exp\left(-\frac{e\phi(x)}{k_B T}\right) \qquad (2.3)$$

Here, N_V is the effective density of states in the valence band, E_a the activation energy of the dopants, k_b Boltzmann's constant, n_A (n_D) the concentration of acceptors (donors) and T the temperature. As can be derived via the Poisson equation, the drain current then depends exponentially on the gate voltage[10]

$$I_D \propto \exp\left(-\frac{e\alpha V_{GS}}{2k_B T}\right) \quad (2.4),$$

where the gate coupling factor α is defined in Equation 5.5. We would like to emphasize that the switching of the FET works without the need of current flowing through the gate insulator but merely by the application of a potential to the gate electrode. This "powerless switching" is one of the reasons why FETs are used in modern electronic devices.

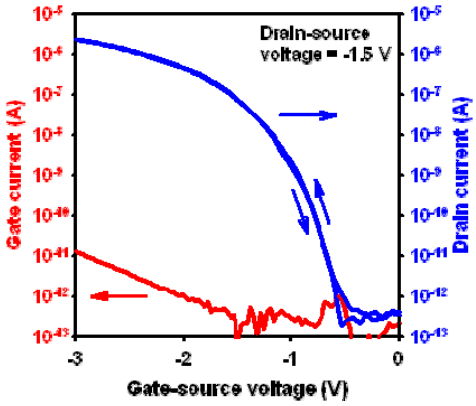

Figure 4 Transfer curve of a field effect transistor. The exponential increase of the drain current between -0.3 and -1 V as well as the vanishing gate current can be seen. In this transistor the semiconducting channel has been fabricated from pentacene molecules [H. Klauk, personal communication].

When the maximal density of charges is accumulated, the maximum drain current I_D flows, and the FET is in its on state (**Figure 4,** at -3 V). Whether it is energetically more favorable for holes or electrons to accumulate in the channel depends on the sign and magnitude of the applied gate voltage as well as on the band gap and doping level of the semiconductor. In turn, obviously if the charge density is minimal, the current through the channel is small and the FET is turned off (-0.2 V in **Figure 4**). For a more detailed explanation of the operation principle of FETs, please refer to references [9, 10].

However, the operation of a FET is not only determined by the density of accumulated charges in the channel. In order for a large current I_D to flow through the device, charges have to be injected into the channel from the source contact. For example, the successful injection of charge carriers from the source electrode into the channel depends on the alignment of the conduction (in the case of an electron channel) or valence (in the case of a hole channel) band with the Fermi level of the metal used for the drain contact. The contact of a metal and a semiconductor leads to a potential barrier (Schotty barrier) that can hinder charge transport across this interface [9]. In case that the channel is composed of an inorganic material, the thickness of the Schottky barrier can be tuned by selective (degenerate) doping of the contacts. In contrast, when organic materials are used, doping is typically not straightforward and special care has to be directed to the choice of the combination of semiconductor and contact metal.

In FETs that are nowadays used in commercial electronic devices, the size of the individual parts of the transistor is beginning to enter into the regime where the wave-nature of the electron is beginning to play a role. For example, the gate insulator of FETs is on the order of few nanometers (**Figure 1** inset) so that one can expect tunneling phenomena of the charge carriers through this insulator already to start playing a role here. In the next chapters we will elucidate the unexpected phenomena that start to appear when electrons get confined to small spaces. We will see that both the wave-nature of the electron as well as the discreteness of the electric charge will strongly be noticeable in the transport processes trough such devices.

3. Transport through a one-dimensional wire

Before we describe the transport of charges trough a one-dimensional wire, let us recall what one dimensional (1D) means. Electrons can be described by wave packages with a wave length given by their energy. In electric transport only the electrons at the Fermi edge (E_F) take part; their wavelength is consequently called Fermi wavelength and is given by $\lambda_f = h/(2m^* E_F)^{0.5}$. If one or more measurement of the device under investigation is smaller than the Fermi wavelength, one can expect the charge carrier to not be able to move into this direction any longer, it gets confined. Typical λ_f in metals are below one nanometer, while they can be up to several tens of nanometers in semiconductors. This is why confinement effects can be seen much easier in semiconductors. Another very crucial value when investigating transport at the nanoscale is the mean free path l_e of the charge carrier. It expresses the distance across which a charge carrier can travel without scattering. As we will see, if the size of a sample is below this size, interesting effects will come about.

The conductivity of a macroscopic sample is typically derived from the Boltzmann equation[11]. It reads

$$\sigma = \frac{ne^2}{m^*}\frac{l_e}{v_F} \qquad (3.1)$$

With n the charge carrier density, e the electron's charge m^* the effective mass of the charge carriers and v_F the Fermi velocity. For copper at room temperature l_e = 30 nm.

What now happens to the conductance of a sample with dimensions significantly smaller than the mean free path? The charge transport then should take place without scattering (this phenomenon is called ballistic transport) and therefore the conductance should rise infinitely. However, experimentally it is found, that the conductance approaches a finite value, the so called conductance quantum $G=e^2/h$. This value does not depend on the material under investigation.

Landauer Formula

The surprising finding that the conductance of a ballistic sample does not rise to infinity can be described with the Landauer formula. This theoretical derivation of the conductance through a ballistic wire holds for non-interacting charge carriers in a ballistic conductor for small biases V_{DS} (called linear response) at zero temperature. Consider a ballistic one dimensional conductor (for this to be true, its width and height should be smaller than the Fermi wavelength of the charge carriers) coupled to two metallic contacts (**Figure 5a**). This means that the allowed energies in y and z-direction are quantized. We consider the conductor to only have one of these quantized energy levels, called a channel, as depicted in **Figure 5b**. A finite bias V_{DS} is applied across this conductor. Since the wire is one dimensional, electrons can only move through the wire from contact 1 to contact 2 in x-direction. The energy of an electron in the lead is given by [12]

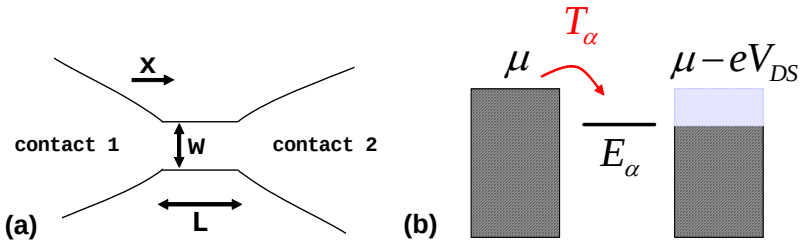

Figure 5 (a) Schematic drawing of a one dimensional wire between two contacts. The length L of the wire is much smaller than the mean free path l_e of the charge carriers, its width is smaller than the Fermi wavelength of the charge carriers. (b) Schematic drawing of the corresponding energy diagram. Shown are the electrochemical potentials of the left (μ) and the right lead (μ-eV_{DS}) across which a voltage V_{DS} has been applied.

$$E = E_\alpha + \frac{\hbar k_\alpha^2}{2m^*}, \text{ with } E_\alpha = \frac{\hbar \pi^2}{2m^* L_y^2} \qquad (3.2),$$

where E_α is the quantized energy of the electron with respect to its transversal motion. The longitudinal velocity v_α of the charge carriers moving in the x-direction is given by

$$v_\alpha(E) = \frac{\hbar k_x}{m^*} = \sqrt{\frac{2}{m^*}(E - E_\alpha)} \qquad (3.3).$$

In order to derive the square-root dependence of v_α we used Equation 3.2.

The current through one channel I_α is then given by

$$I_\alpha = e \cdot T_\alpha \int_{-\infty}^{\infty} D_\alpha(E) \cdot v_\alpha(E)[f(E-\mu) - f(E-(\mu - eV_{DS}))]dE \qquad (3.4).$$

Here, T_α is the probability that a charge carrier is transmitted through the contact into the wire. This transmission probability takes account for a contact resistance like for example a Schottky barrier. The density of states reads

$$D_\alpha(E) = \frac{1}{2\pi}\frac{dk_\alpha}{dE} = \frac{1}{2\hbar\pi}\sqrt{\frac{m^*}{2(E-E_\alpha)}} \qquad (3.5)$$

which can be derived by using the expression for k_α given in Equation 3.2. The Fermi functions f at the end of the formula extract that part of the density of states from which charge carriers can travel from the left to the right lead, as marked in light grey in **Figure 5b**. The current can then be written as

$$I_\alpha = \frac{e^2 \cdot V_{DS} \cdot T_\alpha}{h} \int_{-\infty}^{\infty} (-f'(E-\mu))dE \qquad (3.6).$$

Here we used the difference quotient of the Fermi function

$$\frac{df(E-\mu)}{d(-eV_{DS})} = \frac{f(E-\mu+eV_{DS}) - f(E-\mu)}{-eV_{DS}} \qquad (3.7).$$

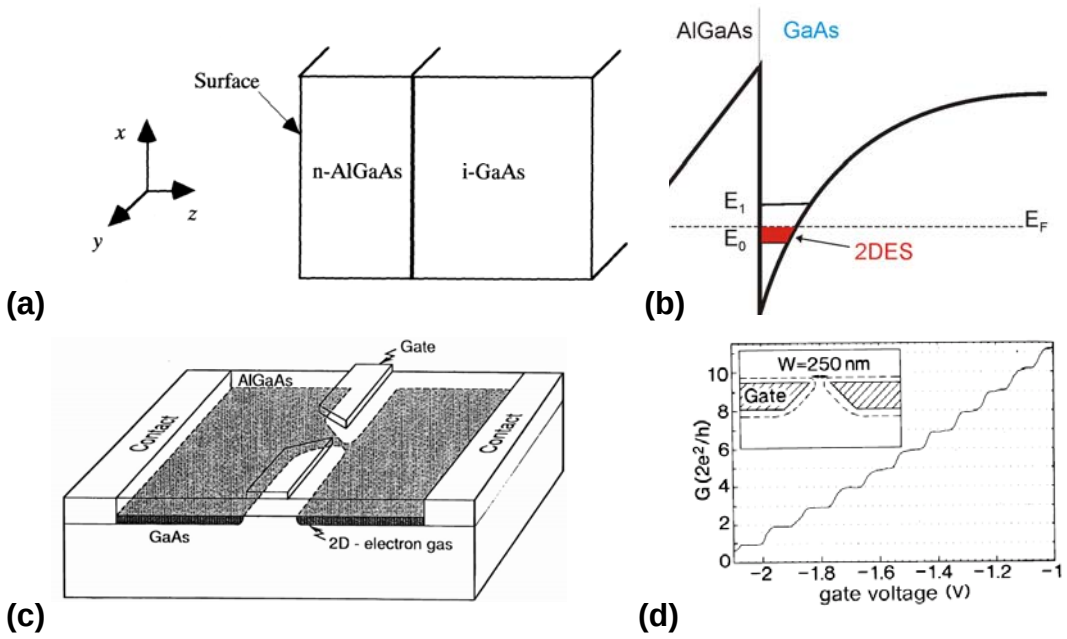

Figure 6 (a) Schematic view of a n-type AlGaAs/intrinsic GaAs interface. (b) Band diagram of the interface region between the two layers. The two dimensional electron gas is formed at the contact between the two layers. (c) Schematic of the experimental realization of a quantum point contact. By application of a negative voltage to the gates, the width of the quantum point contact can be defined (adopted from Ref 1). (d) Conductance through the quantum point contact as a function of the gate voltage (adopted from Ref 6).

Since the integral over the derivative of the Fermi function in Equation 3.6 equals unity for small V_{DS}, the conductance through one channel of the one dimensional wire can be expressed by

$$G = 2 \cdot \frac{I_\alpha}{V_{DS}} = 2 \cdot \frac{e^2}{h} T_\alpha \qquad (3.8).$$

Here we added a factor of 2 to account for the spin of the electron. In the case that the wire is composed of m channels, G increases by a factor m. This derivation showed, that the conductance through a ballistic one dimensional wire is not infinite, but – at a maximal transmission T_α of the contacts of one – an upper limit of e^2/h, the so called conductance quantum. This conductance quantum can be understood as a contact resistance between the ballistic wire and the three-dimensional contact. One can argue that the electrons have to scatter into the one-dimensional channels in order to enter into the wire. In a 4-terminal measurement, the resistance of the ballistic wire really would be zero, as we shall see later when discussing the quantum Hall effect.

Experimental realization of a one dimensional wire

Experimentally, such one dimensional wires can be realized by different methods. One very popular method is the electrostatic confinement of a 2-dimensional electron gas (2DEG, or sometimes called 2 dimensional electron system, 2DES) by electrostatic

gating. A 2DEG is formed at the interface of a AlGaAs/GaAs heterostructure (**Figure 6a**) that is typically grown by molecular beam epitaxy (MBE) methods. The different bandgaps and Fermi levels in the n-doped AlGaAs and the intrinsic GaAs layer lead to the transfer of electrons from the AlGaAs to the GaAs which results in a band bending as shown in **Figure 6b**. The electrons are confined to a very narrow region in the plane of the sample (i.e. the z-direction), which leads to a quantization of the energy in this direction. Typically electrons only occupy the lowest level, so that the motion of the electrons is confined to the xy-plane.
Ohmic contacts can be made to the 2DEG, and two metal gate electrodes with a typical distance of about 250 nm can be patterned on the AlGaAs layer that are electrically insulated from the 2DEG (**Figure 6c**). On the application of a negative voltage to the gates, the 2DEG underneath them is depleted, and as indicated in **Figure 6c,** only a small strip of the 2DEG between the gates is not depleted. The width of the not depleted part of the 2DEG between the gates (the quantum point contact) changes with the magnitude of the applied voltage. As the width of the quantum point contact becomes comparable to the Fermi wavelength of the electrons the density of states in the quantum point contact get quantized and if the size of the level quantization is significantly smaller than the thermal broadening, the current is carried by few one-dimensional channels. Since the quantum point contact fabricated such that it is significantly shorter than the mean free path of the electrons transport through the point contact is ballistic. As the potential applied to the gates is increased, the constriction gets narrower and the number of channels get fewer. This means, that the conductance decreases in a step-like fashion as less and less channels become available for transport (**Figure 6d**).

4. Coulomb blockade

Up to now the interaction between electrons has been neglected and we have considered the contacts to the ballistic wires to be highly transmissive. This chapter will deal with interacting electrons confined to small dimensions and only coupled via tunneling processes to the leads.
In order to understand at which length scales the Coulomb interaction becomes a dominant factor, it is instructive to consider a small metallic particle of diameter *D*. The capacitance of this dot C is given by $C = 4\pi\varepsilon_0\varepsilon_r D/2$. The energy of one additional electron brought onto this dot is given by

$$E_c = \frac{e^2}{2C} = \frac{e^2}{4\pi\varepsilon_0\varepsilon_r D} \quad (4.1)$$

When dealing with macroscopic capacitors, this energy is too small to be measured. As an example, E_c is only about $1\text{x } 10^{-12}$ eV for a 1 µF capacitor. However, as the capacitor gets smaller, E_c increases to measurable values as shown in **Figure 7b**. In order to study the addition and removal of electrons onto such a metallic island, it is frequently coupled via tunneling barriers to metallic leads, as schematically shown in **Figure 7a**. Charges can tunnel onto the dot from the leads and vice-versa with a tunneling rate given by $\Gamma/\hbar$.
In order for single-electron charging events to be visible, the dot has to be weakly coupled to the leads (called the weak-coupling regime). An additional electron can only enter the dot if the Coulomb repulsion is overcome. This is the reason, why for certain

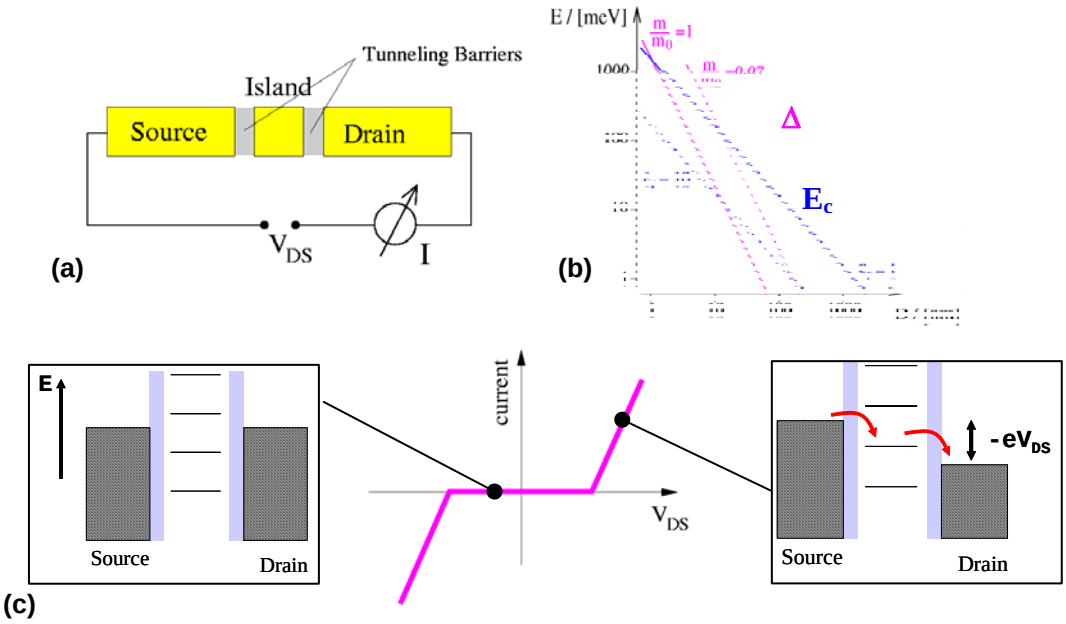

Figure 7 (a) Schematics of a metallic quantum dot coupled via tunneling barrires to metallic leads (b) Energy of one electron on a spherical capacitor E_c and the level splitting Δ plotted against the diameter of the capacitor for two different values ε_r of the surrounding insulating medium. (c) Current flowing through the quantum dot. Current can only flow if an allowed level lies within the bias window opened by eV_{DS}. A schematic energy diagram of the dot in the blockade and in the transport region is shown. Images adopted from J. Weis personal communication

values of V_{DS} no current can flow through the quantum dot due to the Coulomb blockade (**Figure 7c**). Since for each additional electron that wants to enter, the Coulomb repulsion has to be overcome again, it is instructive to visualize the density of states in the quantum dot as discrete values. This has been done in **Figure 7c**. Please note that this level spacing within the dot does not stem from the level quantization due to the quantum mechanical confinement of the charge carriers. However, the quantum mechanical level splitting can lead to an additional splitting of the levels in small dots as we will see later.

When can the Coulomb blockade be seen?

There are two major factors that determine if the Coulomb blockade can be observed in a system under investigation: Firstly, the temperature at which the system is investigated should be sufficiently low so that the thermal broadening is much smaller than the energy of one charge on the quantum dot, that is

$$E_c >> k_B T \qquad (4.2)$$

with T the temperature and k_b the Boltzmann constant. As we have seen from **Figure 7b**, E_c can be much larger than k_bT at room temperature (25 *meV*). However, this is only true for very small quantum dots, so that almost all investigations on quantum dots are performed at cryogenic temperatures between 40 mK and 4 K in a Helium cryostat. The second condition in order for the Coulomb blockade to be visible is that the electron is stable in the dot within the time that it is observed. The timescale is given by $\Delta t = R_t C$

	GaAs quantum dots	10 nm metallic island*	500 nm metallic carbon nanotube	InAs/InP nanowires	molecular transistor
E_C	0.2 to 2 meV	25 meV	3 meV	5 meV	>0.1 eV
Δ	0.02 to 0.2 meV	1 meV	3 meV	<1 meV	>0.1 eV

Figure 8 E_c and level broadening Δ for different material systems. Figure adopted from Ref 4.

with R_t the resistance of the tunnel junction. The condition for an electron to be stable on the dot within Δt is obtained by Heisenberg's uncertainty principle

$$\Delta E \Delta t \approx \frac{e^2}{C} R_t C > h \qquad (4.3).$$

This means, that Coulomb blockade effects will be visible if the resistance of the tunneling junction fulfills the following relation

$$R_t >> \frac{h}{e^2} = 25.8 k\Omega \qquad (4.4)$$

When does the size quantization play a role?

Typical realizations of quantum dots involve small metal islands or quantum dots defined with the aid of electrostatic gates in semiconductor heterostructures. The question then arises, whether the quantum mechanical nature of the electron will lead to a further splitting of the levels in the dot. This is the case when the Fermi wavelength of the electrons is on the order of the lateral dimension of the quantum dot. To a good approximation the potential confining the electrons can be assumed to be parabolic. This yields a level splitting Δ of $\Delta = h^2/2m^*D^2$. It depends on the nature of the dot whether E_c or Δ will be dominant, as shown in **Figure 7b**. Examples of E_c and Δ for different material systems are given in **Figure 8**. In the case that $E_c >> \Delta$ one speaks of a classical dot.

5. Single Electron Transistor (SET)

The position of the energy levels within the quantum dot with respect to the electrochemical potential of the leads can be influenced just like in a conventional field effect transistor by an electrostatically coupled gate electrode. This three terminal device (**Figure 9a**) is called a single electron transistor (SET), since this device can be operated in such a manor that only one electron at a time can pass the quantum dot.

Constant interaction (CI) model

Transport through a quantum dot can be best analyzed within the constant interaction model. For the CI model to be valid, two assumptions have to be made. For one, we assume that the capacitance among the electrons in the quantum dot and those in the environment (e.g. those in the leads) can be described by a single capacitance C.

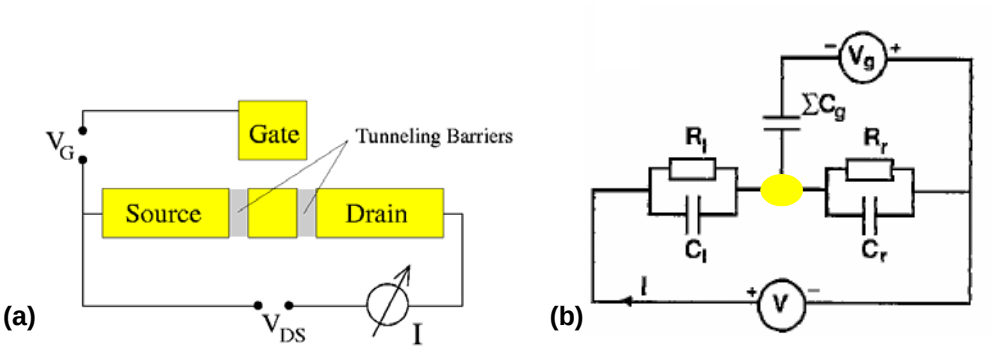

Figure 9 (a) Schematic drawing of a single electron transistor (SET). Image adopted from J. Weis, personal communication (b) Equivalent circuit diagram of a SET. The quantum dot is indicated in yellow.

Furthermore, we assume that C is independent of the number of electrons on the dot. Second, we assume that the single-particle energy-level spectrum as given by Δ is independent of the number of electrons on the dot. In **Figure 9b** the equivalent-circuit diagram of a QD is shown. C_l, C_r and C_g stand for the capacitances between the dot and the drain, the source and the gate respectively. The total capacitance is then given by

$$C = C_l + C_r + C_G \qquad (5.1).$$

The total energy of a dot with N electrons and the voltages V_l, V_r, V_g applied to the respective terminals of the dot is then given by

$$U(N) = \sum_{n=1}^{N} E_n + \frac{(-e(N - N_0) + Q_0)^2}{2C} \qquad (5.2).$$

Here, the first term stands for the sum over the single particle energies E_n that arise due to the size quantization, N_0 is the charge on the dot compensating for positive background charges that might be present in the substrate. Q_0 stands for the effective induced charge on the dot that change its electrostatic potential. It is given by

$$Q_0 = C_l V_l + C_r V_r + C_G V_G \qquad (5.3).$$

The electrochemical potential of N electrons on the dot is then given by

$$\mu(N) = U(N) - U(N-1) = E_N + \frac{e^2(N - N_0 - 0.5)}{2C} - e\alpha V_g \quad (5.4)$$

Here, the gate coupling factor α is given by

$$\alpha = \frac{C_G}{C} \qquad (5.5).$$

The gate coupling factor determines the magnitude of the influence of an external voltage on the electrochemical potential of the dot. The energy difference between two adjacent levels is given by the difference in electrochemical potential between them

$$\mu(N+1) - \mu(N) = \frac{e^2}{C} + \Delta \qquad (5.6),$$

where we used the level spacing $\Delta = E_{N+1}-E_N$. The level spacing can also be zero, if two electrons are added to the same spin degenerate level.

Electron transport trough the quantum dot depends on the alignment of the electrochemical potential within the dot with the electrochemical potential of the leads. The alignment can be established by either applying an appropriate gate or drain-source voltage, as schematically shown in **Figure 10**. In the case that the electrochemical potential levels of the dot do not align with the electrochemical potentials of the lead, the current through the dot is blocked, this is called Coulomb blockade since the electrons do not have suficcient energy to compensate for the Coulomb repulsion that has to be overcome to ener the dot. The blocking of the current is even called Coulomb blockade if the level spacing Δ is dominating e^2/C. If a finite drain-source bias is applied and a level

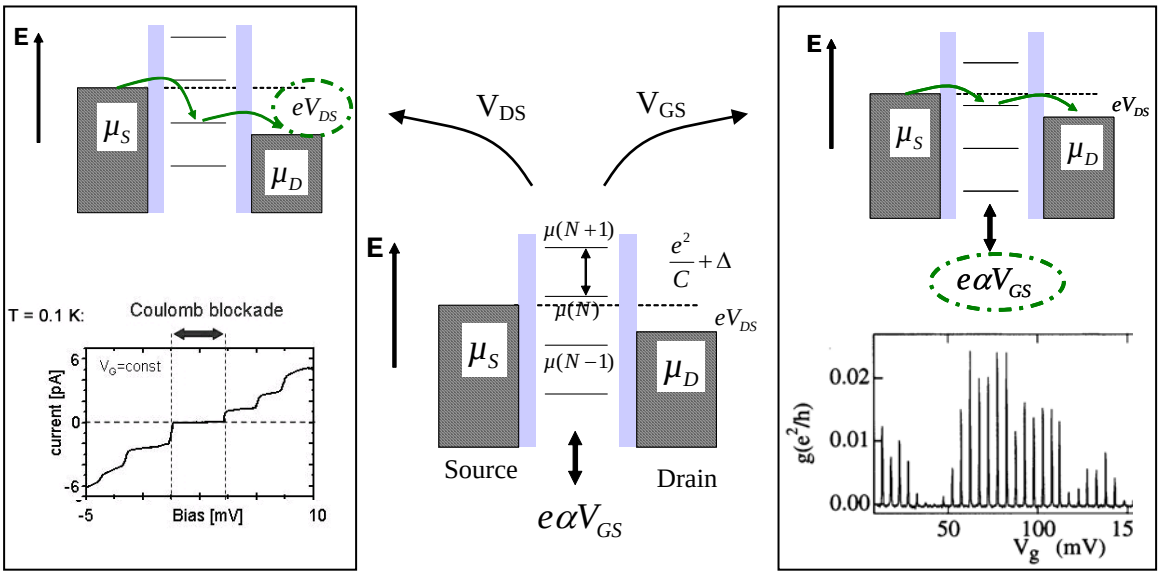

Figure 10 Schematic representation of the electrochemical potential levels of a quantum dot connected via tunnelling barriers to drain and source contacts. Transport through the quantum dot can be realized in two ways: (1) By changing the drain-source voltage (shown on the left) so that a level lies within the bias window opened by eV_{DS}. The current trace is shown in the bottom (image adopted from D. Ralph et al. Cornell University). Each time a further level enters the bias window the drain current suddenly increases. (2) By changing the gate-source voltage so that a level lies within the bias window. (shown on the right) The conductivity then oscillates between a finite value and close do zero, as shown in the bottom (image adopted from Ref 5). These oscillations are called Coulomb oscillations.

enters the bias window that is opened by eV_{DS}, current can flow through the dot, the dot is in resonacne. This process is called sequential tunneling since one electron at a time enters the dot from the drain and leavs it towards the drain. The current increases in a step-like manor (the so-called Coulomb staircase) as a second transport level enters the bias window. While the application of a drain-source voltage only has a very small influence on the chemical potential of the levels on the dot, the gate-source voltage can be used to shift the energy levesl on the dot in energy across wide areas. At small V_{DS} the gate voltage can thus be used to push a energy level into or out of the bias window leading to a high or a supressed current through the dot. These oscillations in the current

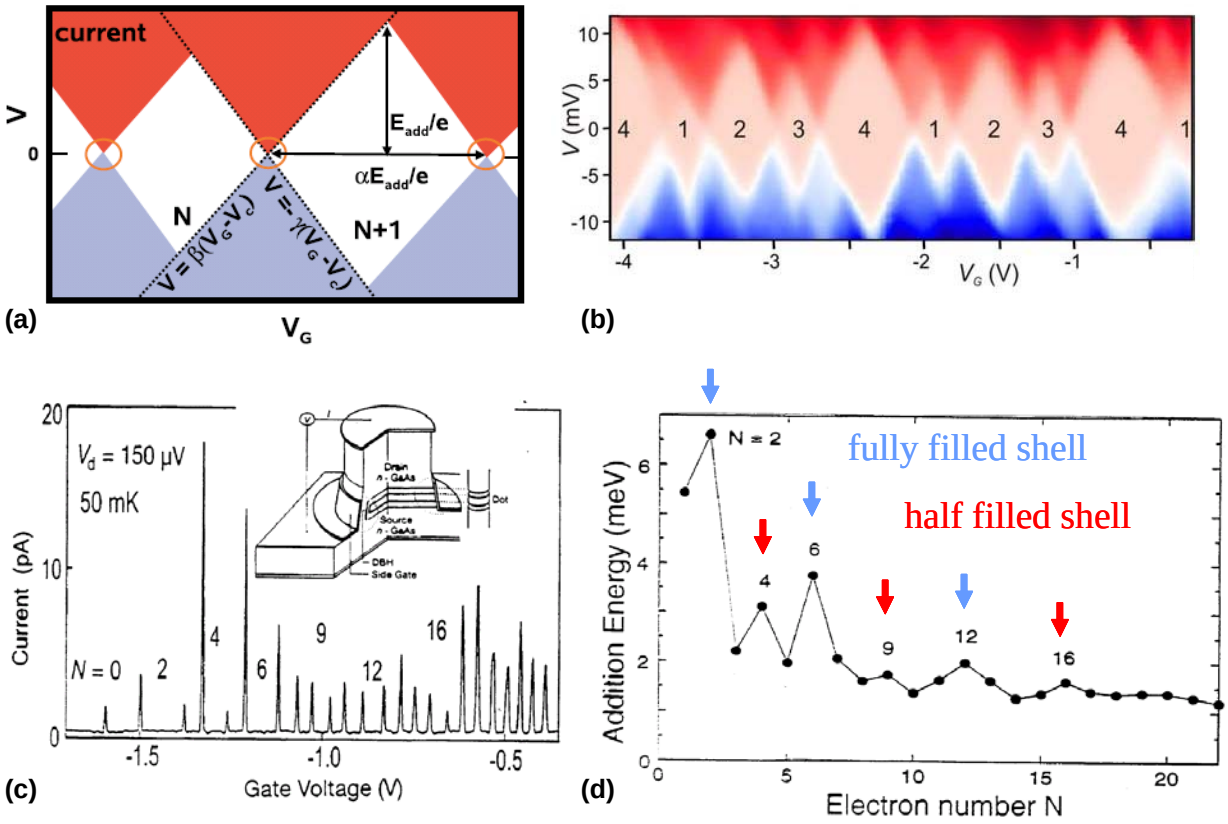

Figure 11 (a) Schematic representation of a Coulomb diamond (stability diagram). For small bias the current only flows in the places indicated (called degeneracy points) (b) Stability diagram for a carbon nanotube quantum dot. Images adopted from Ref 4, (c) Coulomb oscillations as a function of gate voltage for circular semiconductor quantum dot. (d) Addition energy for an additional electron if N electrons are on the dot. Images adopted from Ref 7.

are called Coulomb oscillations. The periodcity of the Coulomb oscillations with the gate-source voltage can be easily calculated from Equation 5.4. If the drain-source voltage is kept constant, the periodicity can be calculated from the following condition

$$\mu(N, V_{GS}) = \mu(N+1, V_{GS} + \Delta V_{GS}) \qquad (5.7)$$

which yields for the periodicity ΔV_{GS}

$$\Delta V_{GS} = \frac{C_G}{eC} E_{add} = \frac{\alpha E_{add}}{e} \qquad (5.8).$$

If the current through the dot is plotted in a two dimensional diagram as a function of the gate-voltage and the drain-voltage, the so called coulomb diamonds emerge, as schematically shown in **Figure 11a**. Each resonance creates two straight lines in the plane that separate the conductive from the non-conductive regions. In the white regions the dot is stable with N, N+1.. electrons and no current flows through the dot. In the colored region current can flow through the dot. The addition energies can be obtained from the height of the coulomb diamonds as well as from the width of the diamonds as shown in **Figure 11a**. In **Figure 11b** an experimental stability diagram from a carbon nanotube quantum dot is shown. The blockade region is shown in pink. The addition of multible electrons to the dot can be clearly seen.

So far we have only considered linear first-order elastic transport processes in which the electrons do not interact with electronic or vibrational excitations. However transport through a quantum dot is also a powerful tool for spectroscopic investigations in order to reveal interactions between vibrations in the system and the conduction electrons. These ineastic tunnel processes have a very distinct signature in the stability diagram[4]. It is noticable in **Figure 11b**, that the addition energy is not the same for all electrons. This is due to the so called shell-filling of the electrons.

Shell structure of a quantum dot –artifical atoms

The difference in addition energy for the Coulomb oscillations shown in **Figure 11c** is depicted in **Figure 11d**. It is clearly visible that the addition of an extra electron to the dot when it is filled with a ceartin number of electrons (N = 2, 6, 12, …) requires a higher amount of energy than for other values of N. This can be understood by remembering that the quantum dot's confining potential can be described by a harmonic potential. This system then is highly symmetric which leads to sets of degenerate single-particle states that form a shell structure just like in an atom. This is why quantum dots are sometimes referred to as artificial atoms. The single-particle energy levels can be calculated from Schrödinger's equation by assuming a harmonic confinement potential given by

$$V(r) = \frac{1}{2} m^* \omega_0 r^2 \qquad (5.9)$$

The stationary Schrödinger equation has the following solutions for the eigenenergies

$$E_{n,l} = (2n + |l| + 1)\hbar\omega_0 \qquad (5.10)$$

with the radial quantum number n = 0,1,2,… and the angular momentum quantum number l = 0,+-1,+-2,…Each shell is filled for the N=2, 6, 12,… for wich the addition energy to add an extra elecron to the dot is maximal.

Experimental realization of a semiconductor quantum dot

A very popular method nowdays of fabricating quantum dots from inorganic materials is a method based on semiconductor heterostructures. The same method as was also used for the fabrication of quantum point contacts is utilized: An AlGaAs/GaAs heterostructure is used as basis material. The 2DEG is depleted electrostatically with the aid of multiple gate electrodes as shown in **Figure 12**.

Applications of single electron transistors

There are a number of applications of SETs, of which three will be briefly mentioned in the following:

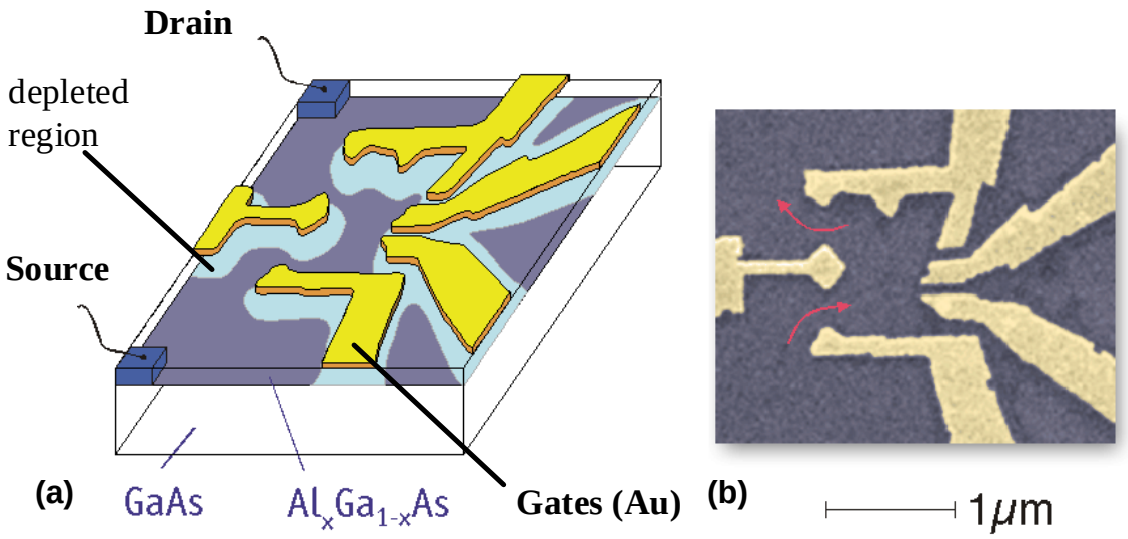

Figure 12 (a) Schematic representation of a quantum dot and (b) an artificially colored scanning electron microscopy image of the experimental realization of a electrostatically defined quantum dot. The tunneling of the electrons into and out of the dot is indicated by the red arrows.

SET as an electrostatic potential probe

The electrochemical potential of the electrons on the dot is very sensitive to electrostatic fields in the close vicinity of the dot. This is why a SET mounted to the tip of a scanning probe microscope can be used to map the electrostatic landscape of a sample with high spatial as well as high energy resolution. For example the potential distribution of a 2DEG in a GaAs sample[13] or the localization of the electrons in the quantum hall effect[14] have been measured with this technique.

SET as a thermometer

Our description of the SET relied on the fact that the temperature of the SET was much lower than the charging energy. However, the width of a Coulomb peak depends critically on the temperature. The width at half maximum of a Coulomb peak depends on the temperature with no adjustable parameters according to the following approximation $V_{1/2} \sim 5.429 k_b T/e$ [Ref 15] Based on this relation, the temperature can be extracted without the need of any system dependent parameters. Temperatures in the range between 20 mK and 1 K can be measured with this technique.

SET for the representation of physical units

The potential use of SETs in metrology stems from the hope to be able to establish a current standard via connecting the electrical charge with the frequency f (and therefore the time) via the relation $I = fe$. Such a relation could be established in a so called single electron pump comprising a SET. The magnitude of the current would be determined via the frequency f. Up to date a working device giving such a current standard has not been realized.[16, 17]

6. Integer Quantum Hall effect (IQHE)

In this chapter the basics of the integer quantum Hall effect will be discussed. This effect was discovered in 1980 by Klaus von Klitzing. For his works he received the Nobel Prize in 1985. It is a further physical effect in which the confinement of electrons to small dimension has surprising effects on the conductivity of a sample under unvestigation.

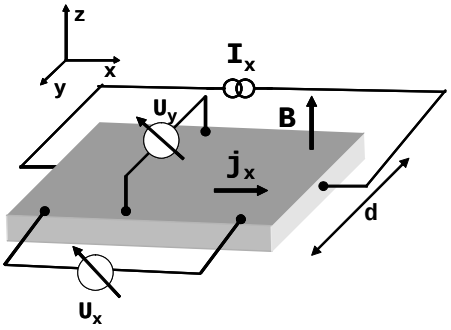

Figure 13 Schematic depiction of typical sample geometry for the measurement of the Hall effect.

Classical Hall effect

Before turning to the IQHE, let us briefly revisit the classical Hall effect, as it is the basis for the unerstanding of the IQHE. If a conductor through wich a current is driven in the x-direction (**Figure 13**) is brought into a magetic field that is directed out of plane (in z-direction), the electrons experience in addition the Lorentz force which diverts them in the y-direction. The stationary Drude equation is then given by

$$\frac{m^*\vec{v}_D}{\tau} = -e(\vec{E} + \vec{v}_D \times \vec{B}) \qquad (6.1).$$

Here the first term on the right side describes the drift of the electrons due to the electric field ***E*** and the second term is the Lorentz force due to the magnetic field ***B***. m* is the effective mass of the electrons, $\boldsymbol{v_D}$ their drift velocity and τ their relaxation time (the mean time between two scattering events). By using the current density

$$\vec{j} = en\vec{v}_D \qquad (6.2)$$

for v_D we can write 6.1 as an expression for the electric field

$$\vec{E} = \frac{m^*}{e^2 n\tau}\vec{j} + \frac{1}{qn}(\vec{j} \times \vec{B}) \qquad (6.3).$$

For the calculation of the magnetoresitivity σ_{xx} and the Hall resistivity σ_{xy} it is viable to express 6.3 in a vector notation

$$\begin{pmatrix} j_x \\ j_y \end{pmatrix} = \begin{pmatrix} \sigma_{xx} & \sigma_{xy} \\ -\sigma_{xy} & \sigma_{xx} \end{pmatrix} \begin{pmatrix} E_x \\ E_y \end{pmatrix} \qquad (6.4).$$

For the general case the conductivity tensor should also include σ_{yy} and σ_{yx}. However, for an isotropic medium and for the applied direction of the magnetic field, $\sigma_{yy} = \sigma_{yy}$ and $\sigma_{xy} = -\sigma_{yx}$. The resistivity in x and y direction are then given by

$$\sigma_{xy} = -\frac{ne}{B}\frac{\omega_c^2\tau^2}{1+\omega_c^2\tau^2} \quad \text{and} \quad \sigma_{xx} = \frac{ne}{B}\frac{\omega_c\tau}{1+\omega_c^2\tau^2} \qquad (6.5).$$

Here, we used the cyclotron frequency ω_c given by

$$\omega_c = \frac{eB}{m^*} \qquad (6.6).$$

The corresponding conductivities are given by

$$\rho_{xy} = \frac{B}{ne} \quad \text{and} \quad \rho_{xx} = \frac{m^*}{ne^2\tau} \qquad (6.7).$$

Please note that as both the conductivity as well as the resistivy are tensors, σ_{xx} is not equal to $1/\rho_{xx}$ and so forth. In the case of a Hall measurement, no current can flow in the y-direction ($j_y = 0$) and therefore Equation 6.4 can be simplified to yield

$$E_y = -\rho_{xy} j_x = -\frac{1}{ne} B j_x = R_H B j_x \quad \text{and} \quad E_x = \rho_{xx} j_x = \frac{m^*}{ne^2\tau} j_x \quad (6.8),$$

where R_H stands for the Hall coeficient. With the Hall effect the charge carrier density n and the type of charge carriers of a sample can be determined.

Landau quantization of a 2DEG in a magnetic field

The integer quantum Hall effect is observed in 2-dimensional electron gases (2DEG) at low temperatures and high magnetic fields. If a 2DEG is brought into a magnetic field, the density of states (which is constant for charge carriers that are confined to two dimensions) splits up into discrete subbands, the so called Landau levels. Their energy can be easily derived from the Schrödinger equation for a free electron that is confined in the z-direction

$$\frac{1}{2m^*}(-i\hbar\nabla + e\vec{A})^2\psi = E\psi \quad \text{where} \quad \vec{A} = (0, Bx, 0) \qquad (6.9).$$

A is the vector potential. Following Landau's ansatz for the wave function we use

$$\psi = \tilde{\psi}(x)\exp(ik_y y) \qquad (6.10).$$

This yields for the energy of the electrons

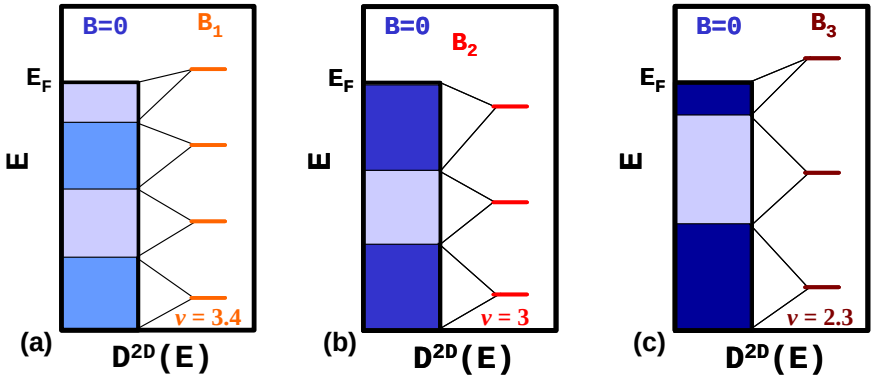

Figure 14 Two dimensional density of states without (left) and with (right) magnetic field. In a magnetic field the density of states condenses onto discrete levels, the Landau levels. The magnitude of the magnetic field increases from (a) to (c). The different shades of blue indicate which states condense onto the same Landau level.

$$E = (l + \frac{1}{2})\hbar\omega_c + E_z \quad (6.11)$$

where we used Equation 6.6 in order to express the so called cyclotron frequency ω_0. This means, that in a magnetic field a two dimensional electron gas will split up into discrete levels spaced by $\hbar\omega_0$ (**Figure 14a**). The degeneracy of each Landau level is given by

$$n_L = \frac{eB}{h} \quad (6.12).$$

Since the degeneracy as well as the spacing between the Landau levels increases with increasing magnetic field, we can expect that with increasing magnetic field less and less Landau levels will be occupied. This effect can be seen in **Figure 14**. The number of filled Landau levels is expressed by the filling factor ν that is given by

$$\nu = \frac{n_e}{n_L} = \frac{n_e h}{eB} \quad (6.13).$$

Here, n_e stands for the charge density of the 2DEG.

Integer quantum Hall effect – experimental realization and phenomenology

A schematic of a typical sample geometry for the measurements of the IQHE is shown in **Figure 15a**. The Hall bar consists of a AlGaAs/GaAs heterostructure that was also used for the fabrication of quantum dots. The 2DEG is confined at the AlGaAs/GaAs interface in the x-y plane of the hallbar. The heterostructure is patterned by etching techniques into the shown hallbar geometry. A light microscopy image of a hallbar structure is shown in **Figure 15b**. The resistances $R_{xy} = U_{xy}/I$ (Hall resistance) and $R_{xx} = U_{xx}/I$ (magneto-

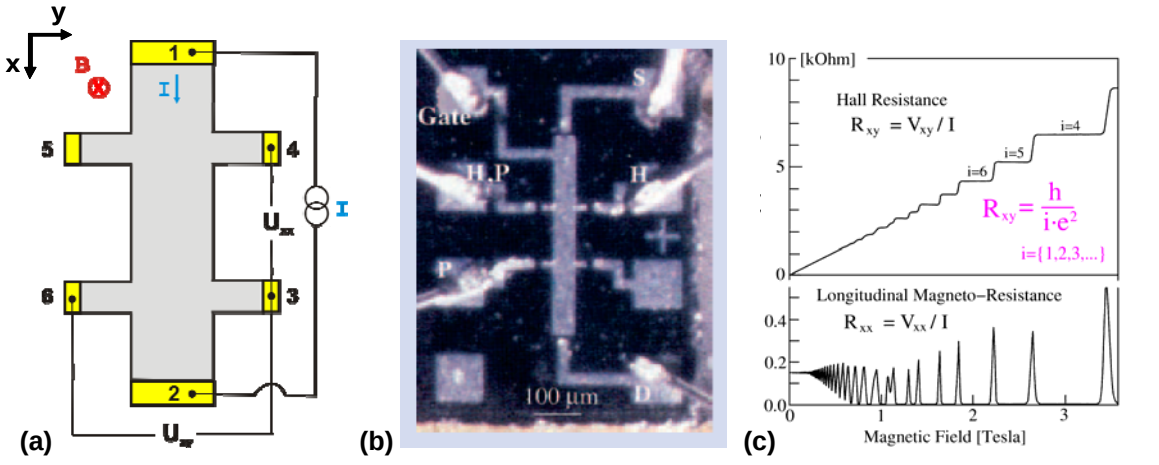

Figure 15 (a) Schematic of a Hall bar geometry. (b) Light microscopy image of a Hall bar. The current ist applied between the contacts labeled by S and D, the Hall voltage (that is proportional to the Hall resitance R_{xy} is measured between the points labeled with H, the longitudinal resistance between points P. (c) Hall and longitudinal resistance of a 2DEG in as a function of applied magnetic field. Images (b) and (c) adopted from Ref 3.

resistance) as a function of the magnetic field is shown in **Figure 15c**. As was derived for the classical Hall effect (Equation 6.7), we can see in **Figure 15c** that for small B R_{xx} depends linear on B and R_{xy} is independent of B.
However, for B higher than a few hunderts of mT, we notice significant deviations from what we would expect for the classical Hall effect: The Hall resistance has distinct plateaus for which the the resistance is a multiple of h/e^2. This is the signature of the integer quantum Hall effect. Since the resistance of the plaeaus can be determined with an exceptional accuracy of 10^{-8}, the quantum Hall effect is used as a resistance standard. Whithin one of the plateaus of the Hall resistance, the magnetoresistance vanishes across a wide region of the magetic field. These oscillations in the longitudinal magneto resistance are called Shubnikov-de-Haas oscillations [12, 18].

The observation that the magneto resistnace vanishes at certain values of the magnetic field can be understood when recalling that the density of states splits up into the Landau levels. With increasing magnetic field the spacing between the individual levels gets larger and their degeneracy also rises. As a consequence with increasing magnetic field more and more Landau levels get depopulated, as was shown in **Figure 14**. Every time all Landau levels are fully occupied (e.i. at integer filling factor) the electrons can move across the sample without scattering, $\tau \to \infty$ and therefore according to Equation 6.7 also $R_{xx}=0$. The reason is, that there are no states for the electrons in the vicinity of the Fermi energy to scatter into. However, this phenomenological explanation can not justifiy why the magneto resistance would vanish across a wide range of the magnetic field. The reason is, that if at integer filling factor the magnetic field is increased, the energetically highest Landau level immediately gets depopulated and therefore empty states that electrons could scatter into would be available. Furthermore, it can not be explained within the now described model why at all current can flow through the sample as there are no empty states at the Fermi level.

Disorder within the sample

The resistance plateaus as well as the extended Shubnikov-de-Haas oscillations can be understood when taking into account that the sample is not free of charged impurities. The effect of these impurities is to broaden the Landau levels as schematically shown in **Figure 16a**. The Landau levels now are divided into localized states in which the electrons are confined to a ceartin area of the sample and can not move across the sample and extended states in the center of the Landau level in which the electrons can move across the sample. The localized states therefore do not contribute to the current but have a influence of the position of the Fermi level. As the magnetic field is increased, the Fermi level can not jump from Landau level to Landau level as it would be the case if the levels were discrete, but remains pinned due to the localized states between the levels. This means, that for an extended region of the magnetic field there exist only fully ocupied extended states but no extended states at the Fermi edge (as the Fermi edge lies within the localized states). This is the reason why the resistance vanishes over wide regions of the magnetic field.

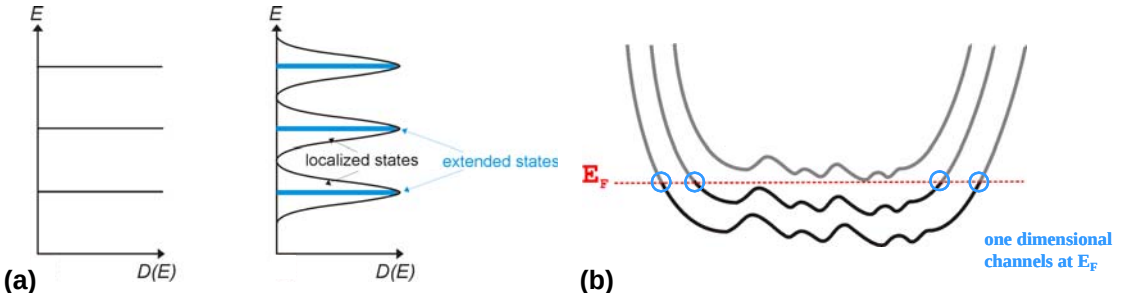

Figure 16 (a) Density of states of a 2 dimensional electron gas in a magnetic field without (left) and with (right) disorder. The presence of disorder within the sample leads to a broadening of the Landau levels. Within one Landau level states exist in which the electrons can move through the sample (extended states) and levels in which the electrons are confined to a certain space of the sample and not free to move through the sample (localized states) (b) Energy landscape of a Hall bar in y-direction. The edges of the sample lead to a strong increase of the energy of the Landau levels at the edges. Within the hall bar the energy landscape has variations due to the disorder within the sample.

However, up to now we still have not explained how the current I flows through the sample and why the Hall resistance takes quantized values. Here the edges of the sample come into play. The edges of the sample can be viewed as an energetic barrier for the electrons. This is why the energy of the Landau levels curves upward in energy at the edges of the sample as depicted in **Figure 16b**. The consequence of this is, that now in each of the Landau levels there is a finite density of states at the Fermi energy at the edges of the sample. Due to the magnetic field the electrons in each of these one dimensional channels are propagating into opposite direction as schematically shown in **Figure 17**. The transport in each of theses channels is ballistic since the spatial division of the two current direction leads to a strong reduction of backscattering of the electrons. This is due to the fact that scattering events that lead to a finite resistance must change the direction of the **k**-vector of the electrons. However, at each side of the sample there are only states available for one **k**-vector so that scattering is strongly supressed. In the case that the Fermi energy in the bulk of the sample is pinned to the localized states and the current only propagates via the edge channels across the sample, the Hall as well as the magnetoresistance can be analyzed in terms of the Landauer formula[12]. Since transport is ballistic within the edge channels, the chemical potentials of the electrodes as marked in **Figure 17** are given by

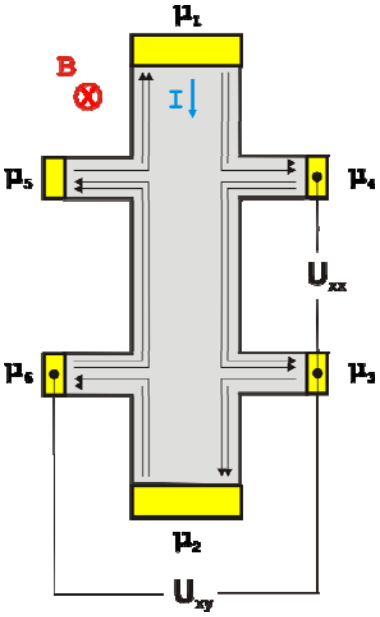

Figure 17 Hallbar in the quantum hall regime. Two edge channels carrying the current are shown.

$$\mu_2 = \mu_5 = \mu_6 \quad \text{and} \quad \mu_1 = \mu_3 = \mu_4 \qquad (6.13).$$

For the respective voltage drops this means

$$eU_{xx} = \mu_1 - \mu_1 = 0 \quad \text{and} \quad eU_{xy} = \mu_1 - \mu_2 \qquad (6.14).$$

The current in a ballistic conductor with n one dimensional current carrying paths is given by

$$I = \frac{e^2}{h} n(\mu_1 - \mu_2) \qquad (6.15),$$

which then leads the values for the Hall and magnetoresistance of

$$R_{xy} = \frac{h}{e^2 n} \quad \text{and} \quad R_{xx} = 0 \qquad (6.16).$$

This picture with the localized and extended states as well as the edge channels can explain the observation of the long range of magnetic field where the Hall resistance remains constant and the magnetoresistance disappears as long as the Fermi level in the bulk remains in the localized states. As soon as the Fermi level enters the extended the electrons can scatter and the magnetoresistance takes a finite value and the Hall resistance makes a jump to a further quantized value.

The IQHE can be also investigated if the magnetic field is kept constant but the charge carrier density is changed, for example by an electrostatically coupled back gate. In fact, the experiments that lead to the discovery of the quantum Hall effect were performed in this manor.

Finally, it is noteworthy, that interactions between the charge carriers have been completely been neglected up to now. However, at high electron densities and high magnetic fields the interaction between electrons gets very strong and leads to the appearance of the fractional quantum Hall effect for which also non-integer steps in the Hall resistance are seen. For a detailed description of this many-body effect the reader is referred to specialized literature[19].

7. References

1 H. v. Houten and C. W. J. Beenakker, cond-mat/0512609 (1996).

2 N. Singh and F. Y. e. a. Lim, in *IEDM* (IEEE, San Francisco, CA, 2006).

3 K. von Klitzing, R. Gerhardts, and J. Weis, Physik Journal **4**, 37 (2005).

4 J. M. Thijssen and H. S. J. Van der Zant, Physica Status Solidi B-Basic Solid State Physics **245**, 1455 (2008).

5 J. A. Folk, S. R. Patel, S. F. Godijn, et al., Physical Review Letters **76**, 1699 (1996).

6 B. J. van Wees, H. van Houten, C. W. J. Beenakker, et al., Physical Review Letters **60**, 848 (1988).

7 L. P. Kouwenhoven, C. M. Marcus, P. L. McEuen, et al., in *Proceedings of the NATO Advanced Study Institute on Mesoscopic Electron Transport*, edited by L. P. K. L.L. Sohn, and G. Schön (Kluwer Series, 1997), Vol. E345, p. 105.

8 D. Kahng and M. M. Atalla, in *Devices Res. Conf.* (Carnegie Inst. of Tech., Pittsburgh, PA, 1960).

9 S. M. Sze, *Semiconductor Devices - Physics and Technology* (Wiley, New York, 2002).

10 R. T. Weitz, (École Polytechnique Fédérale de Lausanne, Lausanne, 2008, Vol. Ph.D. thesis

[11] N. W. Ashcroft and N. D. Mermin, *Solid State Physics* (Cengage Learning Services, 1976).
[12] S. Datta, *Electronic Transport in Mesoscopic Systems* (Camebride University Press, Camebridge, 1995).
[13] M. J. Yoo, T. A. Fulton, H. F. Hess, et al., Science **276**, 579 (1997).
[14] N. B. Zhitenev, T. A. Fulton, A. Yacoby, et al., Nature **404**, 473 (2000).
[15] F. Giazotto, T. T. Heikkila, A. Luukanen, et al., Reviews Of Modern Physics **78**, 217 (2006).
[16] J. Gallop, Philosophical Transactions Of The Royal Society A-Mathematical Physical And Engineering Sciences **363**, 2221 (2005).
[17] K. Flensberg, A. A. Odintsov, F. Liefrink, et al., International Journal Of Modern Physics B **13**, 2651 (1999).
[18] T. Heinzel, *Mesoscopic Electronics in Solid State Nanostructures* (Wiley-VCH, Weinheim, 2003).
[19] T. Chakraborty, *The fractional quantum Hall effect* (Springer-Verlag, New-York, Berlin, Heidleberg, 2002).